This is a preprint. Final version is subject to change. Cite it as:

Giménez-Forcada, E. (2014). Space/time development of seawater intrusion: a study case in Vinaroz coastal plain (Eastern Spain) using HFE-Diagram, and spatial distribution of hydrochemical facies. *Journal of Hydrology* 517, 617–627.

Space/time development of seawater intrusion: a study case in Vinaroz coastal plain (Eastern Spain) using HFE-Diagram, and spatial distribution of hydrochemical facies.

Elena Giménez-Forcada
Instituto Geológico y Minero de España – IGME
Unidad de Salamanca
Azafranal 48
37001 Salamanca, Spain
Phone +34 923260059
Fax +34 923260056
e.gimenez@igme.es

Abstract

A new method has been developed to recognize and understand the temporal and spatial evolution of seawater intrusion in a coastal alluvial aquifer. The study takes into account that seawater intrusion is a dynamic process, and that seasonal and inter-annual variations in the balance of the aquifer cause changes in groundwater chemistry.

Analysis of the main processes, by means of the Hydrochemical Facies Evolution Diagram (HFE-Diagram), provides essential knowledge about the main hydrochemical processes. Subsequently, analysis of the spatial distribution of hydrochemical facies using heatmaps helps to identify the general state of the aquifer with respect to seawater intrusion during different sampling periods.

This methodology has been applied to the pilot area of the Vinaroz Plain, on the Mediterranean coast of Spain. The results appear to be very successful for differentiating variations through time in the salinization processes caused by seawater intrusion into the aquifer, distinguishing the phase of seawater intrusion from the phase of recovery, and their respective evolutions. The method shows that hydrochemical variations can be read in terms

of the pattern of seawater intrusion, groundwater quality status, aquifer behaviour and hydrodynamic conditions. This leads to a better general understanding of the aquifers and a potential for improvement in the way they are managed.

Keywords: Seawater intrusion. Freshening/Intrusion stages. HFE-Diagram. GIS maps.

1. INTRODUCTION

Seawater intrusion occurs in many coastal aquifers around the world. Examples include several coastal areas in Mediterranean countries, where growing population density and human activities drive an increase in water demand. Climate conditions and the scarcity of surface water resources in these areas encourage the overexploitation of groundwaters, usually provoking encroachment of seawater and the concomitant salinization of groundwater. This situation affects water quality and so the development of social and economic activities, as well as potable water supply. Any contribution to understanding this problem is invaluable, and essential if the management of water resources in these areas is to be improved.

Changes in the rates of recharge to, and abstraction from, an aquifer are governed mainly by natural seasonal and inter-annual variations and by global climatic change. Melloul and Collin (2006) link hydrogeological changes in aquifers to rising sea levels, while Masterson and Garabedian (2007) report the effects of rising sea levels on the depth of the seawater-freshwater interface. As Rutulis revealed (1989), renovation of freshwater depends on the aquifer recharge which, in turn, depends directly on the quantity of rainfall and evapotranspiration: as evapotranspiration increases with temperature (a result of climate change), the recharge rate is reduced and this directly affects the water table and groundwater quality (Hoffmann et al. 2000).

Whatever the origin of the problem, it is important to realize that seawater intrusion is a dynamic process, which depends on the temporal variations in the balance of the aquifer

(seasonal and inter-annual periods). These change the position of the interface and cause variations in groundwater chemistry. Therefore, a study of hydrochemical facies and their distribution provides a useful tool in understanding the processes and pathways of seawater intrusion.

Without ruling out other causes, variations in the chemical quality of groundwater in coastal aquifers are controlled by the percentage of seawater present and the participation of secondary processes or water-rock interactions (De Montety et al., 2008). One of the most important secondary processes in alluvial aquifers is cation exchange. These reactions are useful to determine the position and the dynamics of the saline front since, according to whether the ion exchange is direct or reverse, it is possible to identify whether seawater is encroaching (Seawater Intrusion, SwI, or 'intrusion phase') or whether freshwater is rinsing the salinized aquifer (Freshwater Intrusion, FwI, or 'freshening phase'). Water quality can indicate fluctuations in seawater-freshwater mixing, while the dynamics of ion exchange are reflected in changing ionic ratios (Bear 1999).

This study is an attempt to show the relationship between hydrochemical variations and the pattern of seawater intrusion. For that purpose, this study uses concepts from the recently published Hydrochemical Facies Evolution Diagram (HFE-D, Giménez-Forcada 2010). Its results are quantified and translated to map format using a Geographical Information System (GIS). To check its utility and scope, the methodology was applied to a pilot area: the Vinaroz coastal aquifer, which underlies a small alluvial plain on the eastern coast of Spain (Figure 1).

2. THEORETICAL BACKGROUND

2.1. Hydrochemical facies and the seawater intrusion process

The term "facies" has been used in various geological disciplines with varying meanings. In 1838, Gressly was the first to use the term to designate the "aspect" of a group of rocks. Some authors apply the term to eminently descriptive aspects, whilst others use it to refer to generic aspects. Others still, use the term for both types of criteria. Back (1960, 1966)

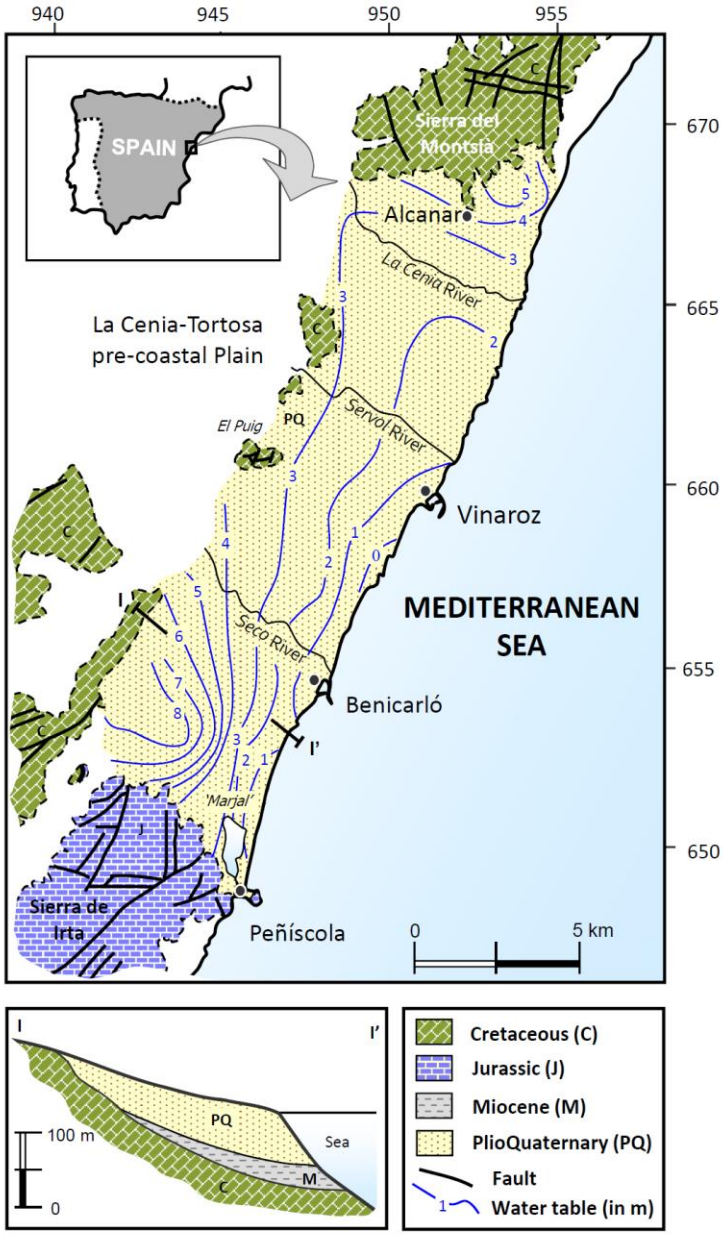

Figure 1. Location of study area: coastal Vinaroz Plain. The limit with the pre-coastal graben of La Cenia-Tortosa Plain is arbitrary and coincides with the threshold of several Crectaceous calcareous outcrops.

took into account the concept of geological facies (meaning similar lithology and depositional history) and defined the term 'hydrochemical facies' to denote "the diagnostic chemical aspect of water solutions occurring in hydrologic systems,'' which ''reflect the response of chemical processes in the lithologic framework and the pattern of water flow in

it''. He applied the idea to groundwater solutes, illustrating for the first time how the solutes changed along a flowpath (in Baedecker and Wood 2009).

In hydrochemistry, the term 'facies' refers to the set of principal chemical characteristics (percentage content of major anions and cations), which defines a water type or group of waters, and which can be interpreted in genetic terms. In 1879, Mojsisovics defined isopic facies, to mean facies that are similar or identical, and heteropic facies, to refer to facies of different rocks in a stratigraphic column. Within this accepted usage of the term, an isopic facies denotes facies with similar characteristics and processes occurring, while a heteropic facies is applied where the characteristics are different, which implies the participation of different processes. This nomenclature can be applied to the concept of hydrochemical facies, which are determined as a function of the percentages of main anions (HCO_3^-, SO_4^{2-}, Cl^-) and cations (Ca^{2+}, Mg^{2+}, ($Na^+ + K^+$)) with respect to the sum of anions and cations (in meq/L), respectively.

A heterotopic or heteropic hydrochemical facies is defined by its own distinct chemical composition, which groups together facies of similar chemical composition or isopic facies (Giménez-Forcada, 2010). Each heteropic facies is represented by a principal facies, defined by percentages of more than 50% of the cation and anion that characterize it. According to these criteria, nine main heteropic hydrochemical facies are recognized (Ca-HCO_3, Ca-SO_4, Ca-Cl, Mg-HCO_3, Mg-SO_4, Mg-Cl, Na-HCO_3, Na-SO_4 and Na-Cl).

Each of the nine heteropic facies mentioned embrace four isopic facies with similar characteristics (i.e., Ca-HCO_3 is the representative heteropic facies, which embraces the four isopic facies MixCa-MixHCO_3, Ca-MixHCO_3, MixCa-HCO_3, and Ca-HCO_3). In the case that no ion exceeds 50%, the type is defined as Mix-ion. The mixed types (MixSO_4, MixHCO_3 MixCl, MixCa, MixMg and MixNa) are described as a function of the dominant anion or cation (see Giménez-Forcada 2010).

2.2. Cation exchange reactions and seawater intrusion dynamics

Cation exchange reactions are a useful tool in the study of the dynamics of seawater intrusion, where the alternation of flows of varying chemical composition (according to the direction of the coastal groundwater flow system) stimulates chemical reactions in the phases of intrusion (saline wedge advancing inland) and freshening (regression of the saline front due to natural recharge).

In the intrusion phase, when saline water penetrates an aquifer previously occupied by fresh water, it produces a reaction that liberates Ca^{2+} and adsorbs Na^{+} in a reverse exchange reaction (Appelo and Geirnaert, 1983):

$$Na^{+} + Ca\text{-}[clay] \rightarrow Ca^{2+} + [clay]\text{-}Na \qquad [1]$$

Direct ion exchange takes place during freshening (or “refreshing”), when a salinized aquifer is flushed by fresh calcium bicarbonate water (Appelo and Geirnaert, 1983):

$$Ca^{2+} + Na\text{-}[clay] \rightarrow Na^{+} + [clay]\text{-}Ca \qquad [2]$$

The reactions that take place are, in fact, far more complex, since numerous factors intervene in the behaviour of the ions (multi-component effect) and this makes it difficult to devise a theoretical description of the phenomenon.

During dry periods, there is a greater need for groundwater exploitation, corresponding to the seawater intrusion stage. Because of its significant salt water content, a small fraction of seawater in the mix dominates the chemical composition of the groundwater. This stage is identifiable through the reverse exchange reaction [1] (Na\Ca) associated with water salinization, a reaction that is assumed to be instantaneous (Kafri and Arad, 1979). Reactions of direct ion exchange [2] (Ca\Na), correspond to the freshening stage, and are generally associated with the wet seasons (usually in spring and autumn in Mediterranean countries)), with relatively long periods of rinsing.

The variations that take place during these two periods could depend on the ratio between the quantity of cations adsorbed onto the solid fraction and their concentrations in solution ($I\text{-}R/I^{i+}$), where I-R represents the ion adsorbed in clay fraction (R) and I^{i+} is the ion in

solution. If the (Ca-R/Na^+) ratio is low, as occurs during the intrusion stage (Ca-R<<Na^+), then the high concentration of sodium in the seawater provokes rapid changes because the quantity of ions (Na^+) in solution greatly exceeds that which can be adsorbed by the aquifer matrix (Ca-R). In contrast, during FwI, the quantity of adsorbed ions (Na-R) is much greater than the input of calcium (Ca^{2+}), so the ratio of adsorbed ions/ions in solution is much higher (in Giménez et al., 1995). In the first case, the concentrations of Na^+ in the mixing water markedly increases with a modest input of seawater. In the second phase the inputs of the calcium ion from the fresh water are low in comparison to the Na-R ions adsorbed. The low calcium concentration in the recharge water can implies that, to produce the same effect as in the intrusion phase, it is necessary for the freshening phase to last much longer, guaranteeing a continuous supply of Ca^{2+} ions. Therefore, the SwI phase is favoured by high ion concentrations and the high salinity of the seawater, while the FwI stage needs more time to become evident.

To better understand these processes, many authors have studied this type of situation by means of laboratory simulations based on the principles of ion chromatography and/or geochemical modelling (Appelo and Willemsen 1987, Appelo et al., 1990, Beekman 1991, Boluda-Botella et al., 2008, Gomis et al., 1996, Gomis-Yagües et al., 1997, 2000, Lambrakis and Kallergis 2001, Appelo and Postma 2005, Lambrakis 2006, Manzano 1993, Martínez and Bocanegra 2002, Xu et al., 1999).

The simulations use columns packed with a solid sample that is in equilibrium with the fluid, occupying the porous media. Appelo and Willemsen (1987) used dilute seawater to simulate the seawater intrusion stage, and obtained profiles that represent the ion concentrations at different instances through the chromatographic column (Figure 2a). Boluda (1994) simulated the evolution of the concentrations of certain ions (Cl-, SO_4^{2-}, Na^+, K^+ and Mg^{2+}) and showed how they increase until they reach the same concentration as in seawater. What particularly stands out from the experiment was the behaviour of calcium: its concentration increases spectacularly due to the Na/Ca ion exchange (Figure 2b). Expression [1] denotes the process in which Ca^{2+} takes part in a reverse ion exchange reaction (Na\Ca):

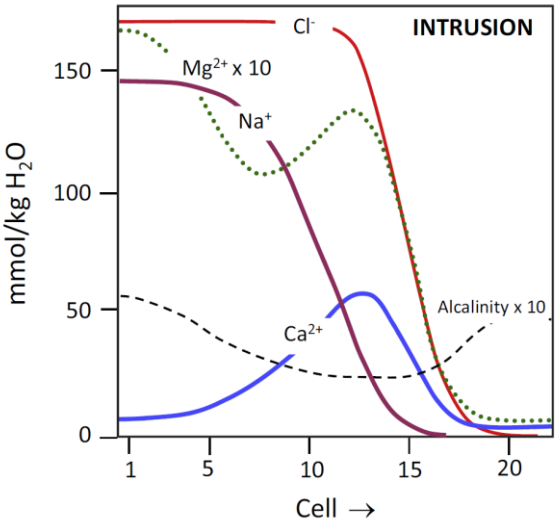

Figure 2a. Simulation of seawater intrusion into a freshwater aquifer occupied, according to model geochemical/mixing cell (according to Appelo and Willemsen 1987; modified).

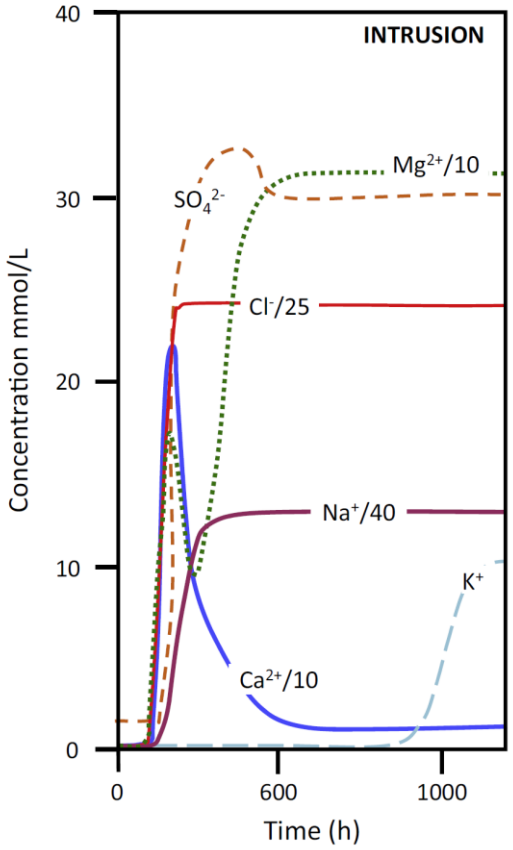

Figure 2b. Evolution of concentration pattern of the major dissolved ions with a flow of 35 mg.min^{-1} of simulation of seawater intrusion (according to Gomis-Yagües *et al*., 1997; modified).

The experiments carried out by Beekman (1991) for the freshening stage offer a model that simulates this process (Figure 2c). The experiment simulates the displacement of all the saline water that was initially held in the aquifer. The simulation entails a series of reactions that sequentially release Na^+ into solution in exchange for Ca, which is retained in the exchange complex. The Ca-HCO_3 waters are converted into Na-HCO_3 facies.

Lambrakis and Kallergis (2001) suggest that when recharge water displaces salt water, the first phase includes a sharp decrease in Ca^{2+}, which corresponds to the dilution of the groundwater behind the saline front.

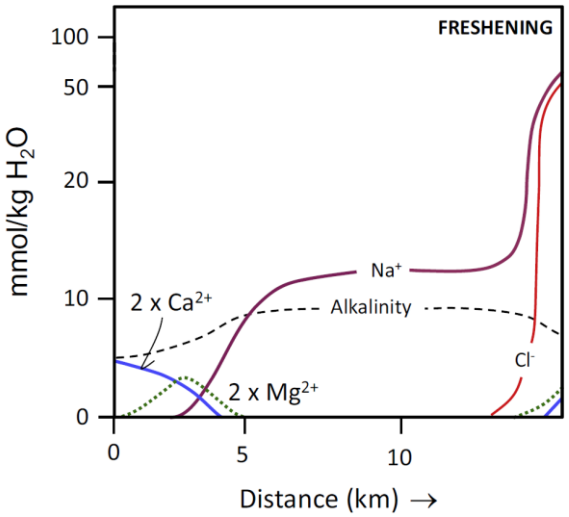

Figure 2c. Simulation of freshwater intrusion into a salinized aquifer (Beekman, 1991; modified).

It can be concluded that both SwI and FwI can be recognized from the hydrochemical facies, particularly from the variation of cation percentage due to cation exchange reactions. Ion exchange seems relatively simple in concept; however, the involvement of all major cations, the lack of detail about the control of selectivity in sediments, and the simultaneous carbonate interactions render the process more complicated than first appears (Appelo and Postma, 2005).

2.3. HFE-Diagram and its utility to create heatmaps

The Hydrochemical Facies Evolution Diagram (HFE-D) provides an easy way to identify the state of a coastal aquifer with respect to intrusion/freshening phases that takes place over time and which are identified by the distribution of anion and cation percentages in the square diagram (Figure 3)[1].

[1] To make the diagram with a common program such as Excel, Grapher, etc., it is necessary bear the following advice in mind: Water samples will be classified according to %Ca and %Na+K, as calcium or sodium waters. For calcium waters (%Ca > %Na+K), the X value will be %Ca+33.3, and for sodium waters (%Na+K > %Ca) the X value will be 100-%Na+K. For the anions, samples will be classified as bicarbonate (%HCO_3 > %Cl) or chloride (%Cl > %HCO_3). For bicarbonate waters, Y values will be %HCO_3-100, and -33.3-%Cl for chloride waters. The X-axis must be represented with a minimum value of 0 and a maximum of 133.3. For the Y-axis the minimum value is –133.3 and the maximum zero.

For representing HFE-Diagram, Excel Macro software is available free by downloading directly from http://hidrologia.usal.es/HFE-D.htm or http://www.igme.es/HFE-D/HFE-D.htm (see Giménez-Forcada, E. Sánchez San Román, F.J. (2014). An Excel Macro to plot the HFE-Diagram to identify seawater intrusion phases. *Groundwater* 2014. DOI: 10.1111/gwat.12280).

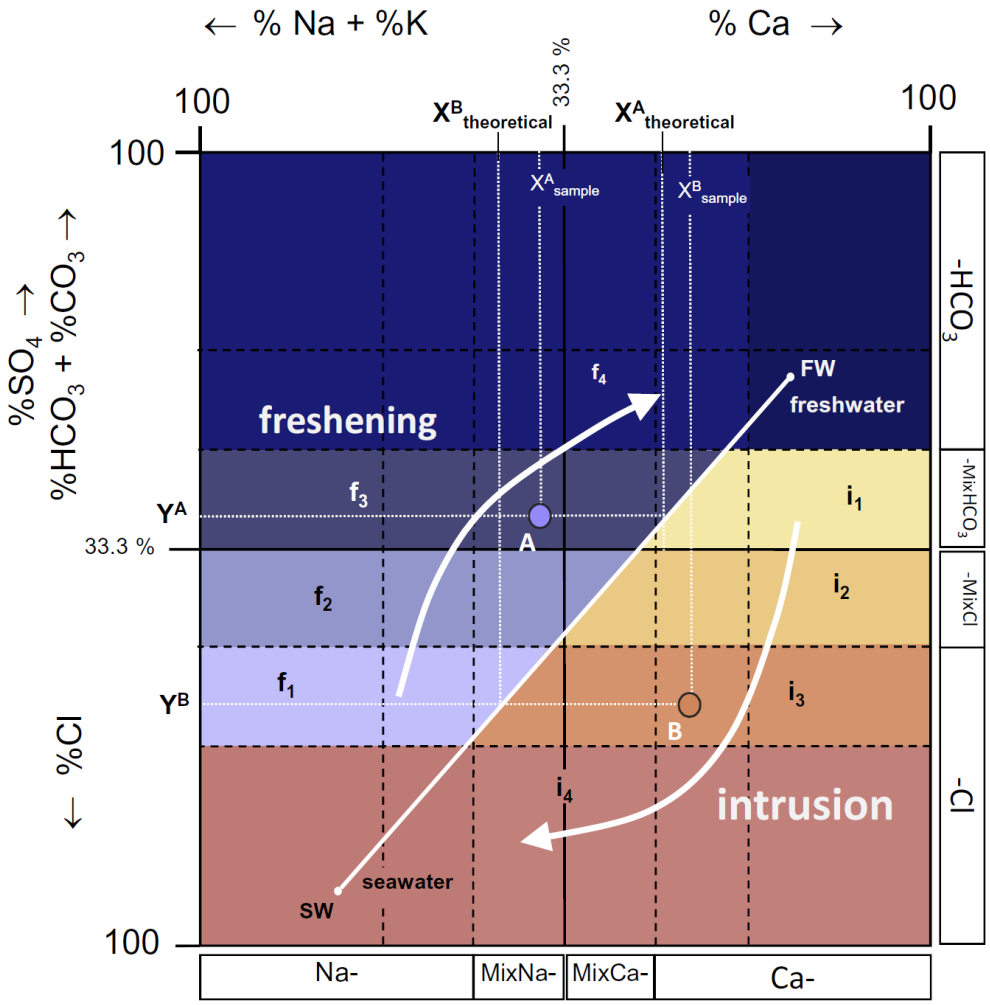

Figure 3. Hydrochemical Facies Evolution Diagram (HFE-D), with the main hydrochemical facies and sub-stages for intrusion and freshening periods. A and B are two examples of waters represented in the diagram, showing how to calculate the differences between the real and theoretical values of X (evaluation of the cation exchange processes).

The X-axis reproduces the line of evolution with two extremes (%Ca and %Na, respectively), which can be interpreted as the evolution of the Na\Ca and Ca\Na exchanges as the calcium and sodium waters mix. The Ca-Cl facies is recognized as the clearest feature of the encroachment of the saline wedge, while the Na-HCO_3 facies (or other isopic facies within this heteropic group) characterizes the complete development of the freshening phase. In other words, when seawater invades the aquifer, the water evolves from a Ca-HCO_3 facies to a Na-Cl one, via an intermediate Ca-Cl facies that is characteristic of the

process (intrusion phase, SwI). This hydrochemical facies is related to reverse cation exchange reactions driven by the sodic water. During the recovery phase, the initial Na-Cl water gradually becomes Ca-HCO3, but this occurs via an intermediate Na-HCO_3 facies or one of the other isopic facies. This characteristic of the freshening phase (FwI) is explained by the direct exchange reactions that drive the increase of Na^+ in the water.

To facilitate the use of the diagram as intended, some ions are not explicitly taken into account in the interpretation (e.g. values calculated relate to the sum total of cations, which includes Mg^{2+}, even though Mg^{2+} is not expressly represented because its participation is secondary (see Giménez-Forcada, 2010, 2011).

In the HFE-Diagram, four heteropic facies are identified: Na-Cl, seawater; Ca-HCO_3, natural freshwater; Ca-Cl, salinized water with reverse exchange; and Na-HCO_3, salinized water with direct exchange. These four facies make up the processes. The facies types situated above and to the left of the Conservative Mixing Line (CML) are representative of FwI, while facies types located below and to the right of the CML represent the SwI stage. Facies types situated in the centre can belong to either the FwI or SwI phases, but this depends on their position compared to the theoretical mixing line (CML) and, therefore, on the chemical composition of freshwater. The composition of seawater used in nthis representation is based on data provided by Drever (1998). The freshwater composition selected corresponds to a theoretical freshwater that takes account of the set of waters represented. For a set of groundwaters, the highest percentages of cation (highest value of %Ca (or %Mg)), and anion (highest value of %HCO_3 (or %SO_4)) in fresh water are chosen. The highest values of %Ca and %HCO3 do not have to correspond to the same water sample; for this reason it is called the theoretical fresh water (it may or may not actually exist). The reason for this is to guarantee that all the samples are represented by one of the two fields that distinguishes the CML in the HFE-Diagram, and which corresponds to the intrusion and freshening phases.

Within the fields of intrusion and freshening, different sub-stages can be identified, following the salinity evolution through the %Cl. In the FwI phase, represented by the top

left curved arrow, the freshening sub-stages (f_1, f_2, f_3, f_4 and FW) can be identified (Figure 3). In the opposite sector of the diagram the SwI sub-stages belonging to intrusion phase are represented (i_1, i_2, i_3, i_4 and SW).

When the aquifer is in the FwI phase, it begins from an initial situation in which the aquifer is totally salinized by seawater intrusion: then, from inland towards the coast, the recharge water begins to rinse the aquifer that is in equilibrium with the Na-Cl facies. The first sub-stage reached is the freshening sub-stage 'f_1' characterized by the distal freshening facies MixNa-Cl. Gradually, the water evolves to sub-stage 'f_2' (MixNa-MixCl) and 'f_3' (MixCa-MixHCO_3, Ca-MixHCO_3), and so to sub-stage 'f_4' identified by the proximal freshening facies 'f_4' (Ca-HCO_3, %Ca<66.6). Finally, the total recovery of the aquifer is identified by the heteropic facies, Ca-HCO_3. As a consequence of direct cation exchange, the X_{sample}-value In all the freshening sub-stages are lower than those corresponding to CML.

In a SwI phase, there is an initial moment when the aquifer is completely filled with 'fresh water' (Ca-HCO_3), which progressively evolves through the following sub-stages. From sub-stage 'i_1', identified by the distal intrusion facies, Ca-MixHCO_3, the water evolves to sub-stage 'i_2' (MixCa-MixCl, Ca-MixCl), and then to sub-stages 'i_3' (MixNa-Cl (50<%Cl<66.6), MixCa-Cl, Ca-Cl) and 'i_4', which is characterized by the proximal intrusion facies MixNa-Cl (%Cl>66.6)). Finally in this phase, the main heteropic facies, Na-Cl, occupies the whole aquifer. All sub-stages of the intrusion period are characterized by higher X_{sample} values than those corresponding to conservative mixing, evidencing the participation of reverse exchange reactions.

Figure 3 illustrates the method used to assign each water sample in the HFE-Diagram to a phase: intrusión ('i') or freshening ('f'). As an example, two water samples (A and B) are represented. Sample A is located in the field associated with freshening, while sample B lies in the field associated with the intrusion phase. In order to calculate numerically whether a sample is in the freshening (A) or intrusion (B) phase, we use the value $X_{theoretical}$ and compare it to the real value of the sample, X_{sample}. The value of $X_{theoretical}$ corresponds to cation and anion percentages on the conservative mixing line, i.e., where there is no

intervention of any cation exchange reaction. If X_{sample} value is lower than $X_{theoretical}$, the water is in a freshening phase (point A); if it is higher, it is in the intrusion stage (point B). The process of calculating ΔC_i utilizes similar comparisons (detailed below).

Having understood this method for associating the position of the samples on the HFE-Diagram to the phases of SwI o FwI, we can see how to identify to which sub-stage it belongs, as a function of the percentage of chloride. Table 1 lists the criteria for differentiating these sub-stages for every phase, and how to quantify and then transfer these results to a map. The following method was chosen to quantify the phase and the sub-stage: The lowest value (1) is assigned to freshwater and the maximum (10) to saltwater. For freshening sub-stages f_4, f_3, f_2 and f_1, the values increase from 2 to 5; then the intrusion sub-stages i_1, i_2, i_3, i_4, go from 6 to 9, ending with saltwater (10). The value 5.5 would represent the boundary between the two stages.

The GIS and spatial plots are used to show the spatial distribution of the freshening and intrusion facies or sub-stages identified in the HFE-Diagram. For this purpose, each water point is geo-referenced and associated to a Z-value, representative of every phase and sub-stage identified in the HFE-D.

The analysis is carried out using *ArcView spatial analyst* and the spline method, which is an interpolation procedure that fits a minimum - curvature surface through the input concentration of each well.

Table 1. Summary of criteria to assign a numerical value to each sub-stage.

substage	anion facies	Ion percentage	cation exchange evaluation	Value	Range in heatmap	Colour
freshwater	$-HCO_3$	% HCO_3 > 50% %Ca >66.6%	-	1	≤2.5	
f_4	$-HCO_3$	% HCO_3 > 50%	$X_{sample} < X_{theoretical}$ freshening	2		
f_3	$-MixHCO_3$	50% ≥ %HCO_3 > 33.3%		3	2.6-3.5	
f_2	-MixCl	33.3% < %Cl ≤ 50%		4	3.6-4.5	
f_1	-Cl	50% < %Cl < 66.6%		5	4.6-5.4	
boundary				5.5	5.5	
i_1	$-MixHCO_3$	50% ≥ %HCO_3 > 33.3%	$X_{sample} > X_{theoretical}$ intrusion	6	5.6-6.5	
i_2	-MixCl	33.3% < %Cl ≤ 50%		7	6.6-7.5	
i_3	-Cl	50% < %Cl < 66.6%		8	7.6-8.5	
i_4	-Cl	%Cl > 66.6%		9		
saltwater	-Cl	%Cl > 66.6% %Na> 50%	-	10	>8.5	

The results are shown on heatmaps, which provide a distribution of hydrochemical facies in a general process of seawater intrusion. The method was applied to the Vinaroz Plain data.

3. SETTING OF THE PILOT AREA

The Vinaroz Plain is an alluvial plain aquifer about 120 km^2 in extent, located on the Mediterranean coast. It occupies a coastal strip approximately 25 km long (Fig. 1).

The average altitude varies from 0 m on the coast, to 100 m at the western boundary of the plain. The Vinaroz Plain is crossed by several intermittent rivers (La Cenia, Servol and Seco), which are dry for most of the year, flowing only after periods of intense rainfall.

The northern plain is in contact with the Sierra de Montsià mountain range, whilst its southern edge borders the Sierra de Irta range. The Mediterranean Sea forms the limit to the east. To the west, the pre-coastal La Cenia-Tortosa plain is in direct contact with the Vinaroz plain through an open border interrupted by several small hills (e.g. El Puig in Fig. 1) which divide the connection between the pre-coastal plain and Vinaroz coastal plain into two sectors: the northern sector is associated with the river La Cenia and the southern part to the river Seco.

Geologically the plain is a tectonic graben, limited to the north and south by Mesozoic uplifts. The most important Jurassic outcrops are located to the south, in the Sierra de Irta range. To the north and west of the plain, the Cretaceous outcrops form the main upland reliefs of the area. Hydrogeologically, the plain is an alluvial aquifer formed by lenticular beds of gravels, sands and clays, with little vertical or lateral continuity, and frequent lateral changes of facies. The thickness of the main aquifer is variable, increasing progressively towards the shoreline, where it reaches 100 m.

From the hydrogeological point of view there are three different formations on the Vinaroz Plain (see cross-section in Fig. 1): (i) upper detrital formation (Plio-Quaternary unconfined aquifer of the Vinaroz Plain (PQ)); (ii) loams and clays in the middle formation

(Miocene set (M)); and (iii) deep limestone package belonging to the lower formation (Mesozoic basement, Jurassic (J) or Cretaceous (C)). The middle formation (Miocene) is considered as an impermeable barrier between the Plio-Quaternay aquifer and the Mesozoic basement (IGME 1988). The hydraulic connection between the groundwaters in the different formations or sub-aquifers and the sea is not well understood.

The hydraulic characteristics of the phreatic aquifer are highly variable. In general, transmissivity ranges from 300 to 1000 m^2/day, but it depends on the thickness of the Mio-Quaternary formation, which is higher in the northern sector. The storage coefficient ranges from 5 to 10%. Recharge occurs from direct infiltration, irrigation return water, and above all, from lateral recharge (from the Mesozoic aquifers and from La Cenia-Tortosa Plain). Outflows occur as underground discharges to the sea, pumped abstractions and flow into the underlying Miocene and Mesozoic aquifers (Diputación de Castellón-IGME 1988, Navarrete et al. 1988).

In inland areas, the piezometric table remains above sea level, whilst in the coastal strip the levels are close to sea level or sometimes even below. The disposition of the isopiezometric lines gives some idea of the recharge of the detrital aquifer from the neighbouring aquifers, both carbonate (Jurassic or Cretaceous) alluvial aquifers (La Cenia-Tortosa Plain), although the direction of the recharge flow is variable. In the most northerly sector, the preferential direction is N-S, indicating inflows principally from the Sierra del Montsià range. Towards the south, this direction shifts towards the W-E, coinciding with the open connection with La Cenia-Tortosa pre-coastal plain. On the southern part of the plain the groundwater recharge flows W-E, from the Cretaceous outcrops of the foothills of the Sierra de Irta. The isopiezometric contours in the southern and northern sectors indicate significant differences in hydraulic gradient: the hydraulic gradients are lower in the north and higher in the south (in Giménez-Forcada 2008).

According to previous studies (IGME 1982, Giménez and Morell 1988, Giménez 2003, Giménez-Forcada 2008), the Vinaroz Plain aquifer exhibits salinization processes that are the result of seawater intrusion, provoked by intensive groundwater abstractions, particularly

along the coast. Salinization is a problem along the coastal strip, specifically close to the towns of Vinaroz, Benicarló and Peñíscola. The remainder of the aquifer does not suffer to any significant degree from salinization.

The recharge waters are of the type Ca-HCO_3. There is significant lateral recharge into the coastal plain over its northern and southern continental boundaries, and this is evidenced by the Ca-HCO_3 recharge waters that are recognised – at times, occurring very close to the coastline. The most saline waters occur near the coast and are characterized by elevated concentrations of calcium and relatively low concentrations of sodium, taking the chloride concentrations as the conservative reference ion.

Calculation of ionic deltas (ΔC_i) is useful to identify ion exchange processes (Fidelibus et al., 1993, Giménez et al., 1995; Pulido Lebeouf 2004; Appelo and Postma 2005). Ion concentrations in the water samples ($C_{i,\ sample}$) are compared with those resulting from theoretical mixing between fresh- and seawater ($C_{i,\ FW\text{-}SWmixing}$). Differences between the observed and expected concentrations are expressed as ΔC_i (in meq/l).

$$\Delta C_i = C_{i,\ sample} - C_{i,\ FW\text{-}SWmixing}$$

To calculate the theoretical concentration of each ion, it is necessary to determine the fraction of seawater f_{SW}, which is defined as:

$$f_{SW} = (C_{Cl,\ sample} - C_{Cl,\ FW}) / (C_{Cl,\ SW} - C_{Cl,\ FW})$$

where $C_{Cl,\ sample}$ is the Cl concentration in the sample; $C_{Cl,\ FW}$ is the freshwater Cl concentration, and $C_{Cl,\ SW}$ is the Cl concentration in seawater.

The following expression is applied to find the theoretical concentration of each ion:

$$C_{i,\ FW\text{-}SWmixing} = f_{SW} \cdot C_{i,\ SW} + (1\text{-}f_{SW}) \cdot C_{i,\ FW}$$

These calculations are valid because Cl can be considered as a conservative tracer.

ΔC_{Na+K} and ΔC_{Ca} values for chloride waters are reported in Figure 4, where water samples are ordered according to increasing chloride concentration. This figure shows participation of exchange reactions in the chemical character of groundwaters. The high

values of ΔC_{Ca} are accompanied by low ΔC_{Na+K} values in the most saline waters in the intrusion phase. In less saline water, the ΔC_{Na+K} is positive and associated with negative ΔC_{Ca} and this is interpreted as an indicator of the freshening phase.

Regarding the general distribution of hydrochemical facies over the Vinaroz Plain, the hydrochemical facies evolves from Ca-HCO_3 to Na-Cl or Ca-Cl, approaching the coast, with the CaCl facies occurring particularly near the largest coastal towns of Vinaroz and Benicarló. In Peñíscola, salinization is controlled in part by the marsh area (Marjal), which is a small long-standing lagoon, separated from the sea by a sand and gravel dune barrier. This area is located near the town of Peñíscola, well known for its tombolo.

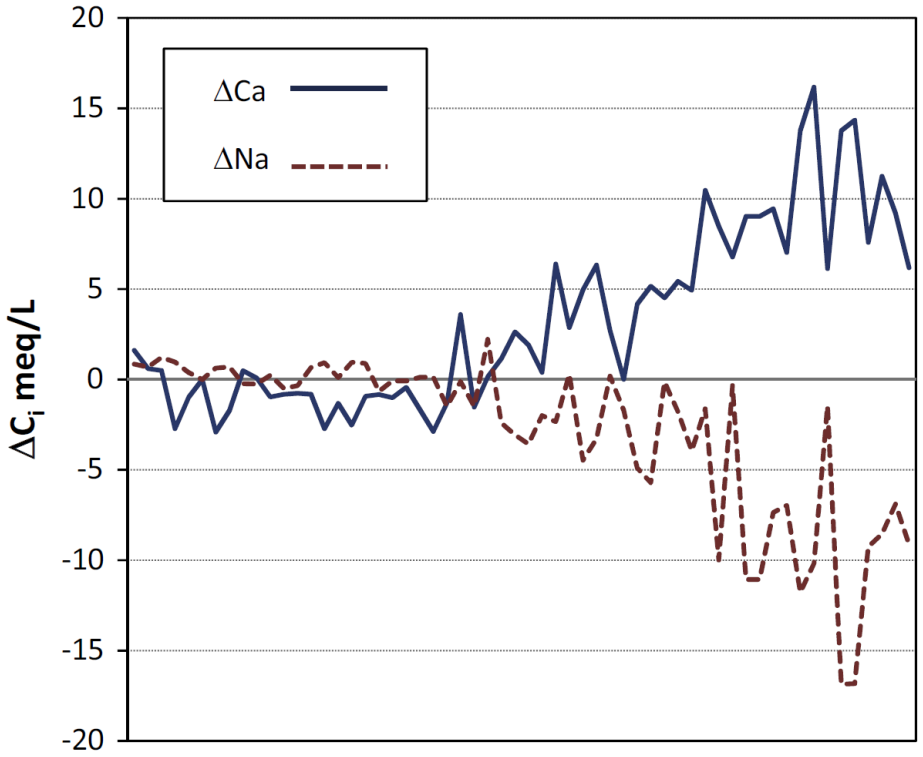

Figure 4. Trends of ΔC_{Na+K} and ΔC_{Ca}. The samples are ordered according to increasing chloride concentration.

In terms of the dissolution and precipitation of calcite, all the water samples were subsaturated in calcite, with $SI_{calcite}$ ranging from -1.48 to -0.66. No difference is seen between the FwI and SwI phases. No sulphate reduction was detected. Concentrations of SO_4 range from 8.6 mg/L - 490 mg/L), with a median of 144 mg/L.

With respect to other contaminants, water quality is affected by nitrate pollution linked to the use of fertilizers for citrus and vegetable crops; nitrate concentrations in groundwaters are high (>50 mg/L (in Giménez, 2003). This pollution has not been considered in this study. The values of NO_3 have not been taken account in the representation of water samples in the HFE-Diagram.

The general hydrochemical characteristics of the Vinaroz Plain, described above, and the geographical distribution of water facies from inland to the coast, led to its selection as a pilot area to test the application of the methodology proposed in this paper.

4. MATERIALS AND METHODS

To determine the aquifer state in a given moment, water samples were selected from three sampling periods (July 1990, November 1990, and December 1992). From the July 1990 period, 21 samples regularly distributed over the study area were considered, and 17 sampling wells in November of that year. To determine inter-annual variations, 20 wells sampled in December 1992 were selected. Even though water points do not always coincide in the three sample periods, in all cases, there is a homogeneous distribution of water samples over the aquifer.

Most of the wells are used for irrigation purposes and possibly for potable supply. They range from 20-100 m of depth. On occasions, there is no information about the characteristics of the water point regarding depth or use; this means that it is possible that the exploited aquifer is deeper (e.g. Miocene/Mesozoic basement). This could be true for several boreholes located in the surroundings of Vinaroz and Benicarló, where salinization is almost continuous. The salinization may also be due to continuous pumping of the boreholes to supply these towns.

On-site analysis included water temperature, pH and EC (electrical conductivity at 25°C). At each site, water samples were also collected for laboratory analysis. Samples were collected on site into factory-new polyethylene bottles, refrigerated at 4°C for later analysis in the laboratory. Calcium, Mg and Na were measured using AAS (Atomic Absorption

Spectrophotometry), K was determined by FES (Flame Emission Spectrometry). Alkalinity (HCO_3) was determined by volumetric titration, while chloride was analysed by Mohr titration. Sulphate content was determined according to the barium sulphate turbidity method, and nitrate concentration by the UV Spectrophotometry Method. The analytical techniques used to determine the chemical parameters were taken from Standard Methods for the Examination of Water and Wastewater (APHA, AWWA, WPCF 1989). All analyses are believed to be accurate to within ±2.0%. In all cases, electrical charge imbalances were less than 3%. Table 2 show the descriptive statistics of the physico-chemical parameters for the three sampling periods analysed (July 1990, November 1990 and December 1992).

Table 2. Descriptive statistics of the physicochemical parameters for the three sampling periods (July 1990, November 1990 and December 1992). The data are expressed in µS/Cm for EC and in mg/L for TDS, major and minor ions.

JULY 1990	EC	TDS	HCO_3	Cl	SO_4	NO_3	Ca	Mg	Na	K
Mean	2394	1623	267.8	554.1	148.1	139.9	200.9	60.23	231.4	6.44
Median	1660	1126	256.2	252.0	120.0	124.0	174.0	37.67	103.5	3.99
Std error	473.4	269.6	12.86	143.1	27.87	21.42	24.69	10.97	61.82	1.41
Std Dev.	2169	1236	58.95	655.6	127.7	98.14	113.1	50.28	283.3	6.46
Minimum	580.0	528.3	122.0	28.40	19.20	18.60	68.00	14.58	13.80	0.50
Maximum	6940	4092	372.1	2016	489.6	378.2	448.0	182.2	963.7	23.9
Count	21	21	21	21	21	21	21	21	21	21

NOVEMBER 1990	EC	TDS	HCO_3	Cl	SO_4	NO_3	Ca	Mg	Na	K
Mean	2054	1493	144.9	551.9	147.4	185.3	151.5	58.82	232.7	6.13
Median	929.0	634.3	128.1	177.5	81.60	105.4	92.00	32.81	59.80	0.50
Std error	486.8	335.6	14.39	168.4	27.46	36.58	27.14	13.63	71.32	1.79
Std Dev.	2007	1384	59.32	694.4	113.2	150.8	111.9	56.22	294.1	7.40
Minimum	425.0	379.4	61.00	35.50	24.00	18.60	42.00	6.080	25.30	0.500
Maximum	6030	4105	311.1	1988	379.2	489.8	414.0	184.7	920.0	19.9
Count	17	17	17	17	17	17	17	17	17	17

DECEMBER 1990	EC	TDS	HCO_3	Cl	SO_4	NO_3	Ca	Mg	Na	K
Mean	1983	1397	217.7	460.8	111.6	152.8	164.3	62.47	203.5	5.65
Median	1555	1117	230.6	243.2	86.16	126.5	149.4	42.89	65.32	1.60
Std error	363.5	242.2	16.17	120.0	18.86	25.21	22.36	10.82	56.60	1.68
Std Dev.	1625	1083	72.31	536.7	84.35	112.7	100.0	48.40	253.1	7.50
Minimum	462.0	376.8	97.60	26.27	8.640	20.46	45.60	10.21	9.200	0.500
Maximum	5560	3535	329.4	1596	288.0	374.5	399.2	198.9	855.6	29.9
Count	20	20	20	20	20	20	20	20	20	20

The percentages of cations and anions were calculated using meq/L values, with respect to the sum of cations and anions, respectively. To represent cation percentages on the X axis of the HFE-Diagram, water samples were divided into calcium (or magnesium) waters [%Ca (or %Mg)>%(Na+K)], and sodium waters [%(Na+K)>%Ca(or %Mg)], while to represent anion percentages on the Y axis, samples must be divided into bicarbonate waters [%HCO_3(or %SO_4)>%Cl] and chloride waters [%Cl>%HCO_3(or %SO_4)]. X and Y values in the HFE-Diagram need to be calculated based necessarily on this division. Afterwards, each group of water was treated differently when calculating the values of X and Y (see the explanation offered in the footnote on page 9).

5. RESULTS AND DISCUSSION

The water samples are represented in the Piper diagram (Figure 5). In general, water samples oscillate between bicarbonate and chloride facies (for anions), and between sodium and calcium (or sometimes magnesium) facies (for cations). However, there are no significant differences between the three sampling periods.

For July 1990 and December 1992, water chemistry is more variable, both for anions and cations, with the variation being slightly less for waters collected in November 1990. In the diamond field, the samples vary from sodium chloride facies to calcium bicarbonate facies, passing through intermediate facies, such as calcium chloride facies.

The chemical differences between samples collected on different dates and in different locations are better represented in the HFE-Diagram, which avoids amalgams (sum of percentages) and so better distinguishes the hydrochemical facies. In figure 6, all samples belonging to the three sampling periods are represented in the HFE-D along with the CML for seawater and freshwater. In the HFE-D, 58.6% of samples are located in the intrusion field, where the characteristic facies reaches Ca-Cl (%). The recharge of the aquifer with Ca-HCO_3 water seems insufficient for direct exchange reactions to occur and reach the next facies in the Na-HCO_3 freshening phase. More distal facies might be the only ones that represent the freshening process, though these might not be isopic facies of the Na-HCO_3

facies. On the Vinaroz Plain, for the periods analysed, the most representative freshening phase is the MixNa-MixCl facies.

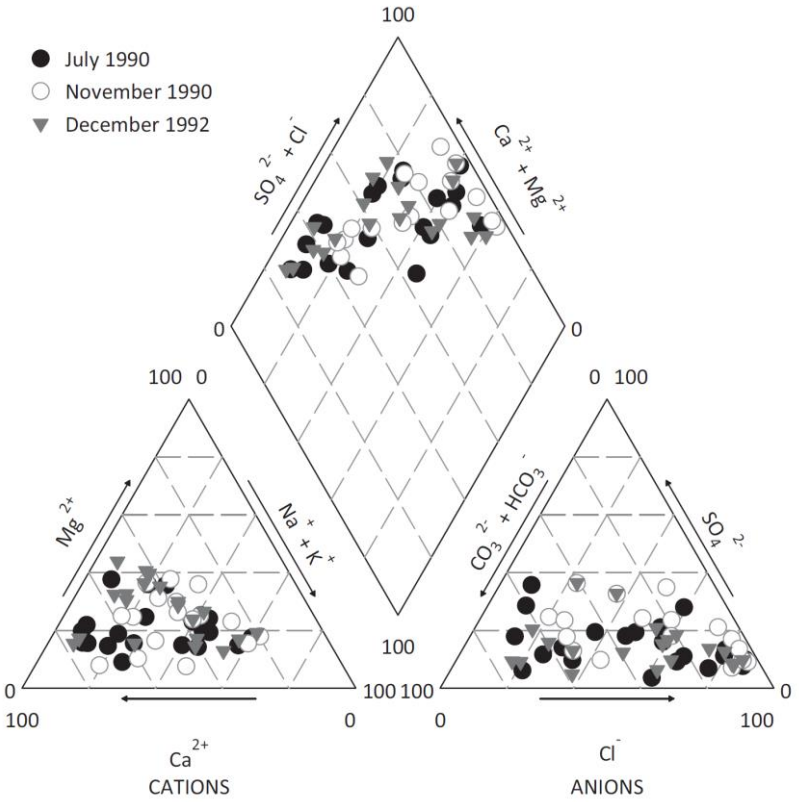

Figure 5. Representation of waters sampled in July and November 1990, and December 1992 in the Piper diagram.

On the right of the diagram, the percentage of anions is correlated with the salinity of the water, by means of the representation of EC in the abscissa. Usually, waters in freshening sub-stages have lower EC values than those corresponding to intrusion sub-stages.

The position of each sampling point in the diagram was quantified and the values transferred to map format to show the distribution of the phases and their respective sub-stages for each sampling period. In Figures 7a, 7b, and 7c, GIS-maps show the distribution of facies for the three dates considered.

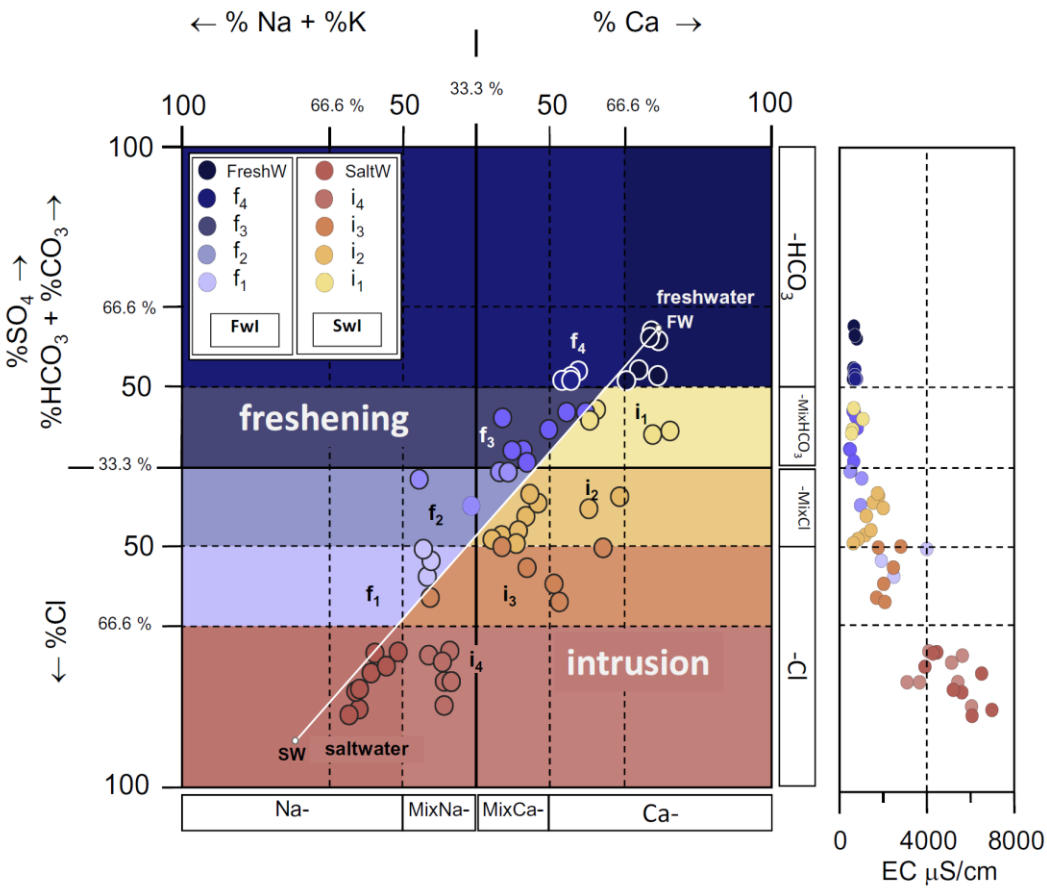

Figure 6. Representation of all water samples on a HFE-Diagram, taking account of their position in relation to intrusion and freshening substages and CML. On the right, the samples have been represented in terms of their electrical conductivity (EC) values.

The 'spline with barriers' method (in this case study, the barrier was a shape-file with the contour of Vinaroz Plain) of spatial analysis was used to the interpolation. The output cell size selected was the same for all cases, and the smallest of the three dates considered.

The sub-stages i_1 and f_1 represent the distal facies of intrusion and freshening, respectively, and establish the position of the boundary between both processes. The boundary must not be mistaken with the conservative mixing line (CML), represented in the HFE-Diagram, nor with the saline wedge (as understood until now). What is shown is the aquifer reaction with respect to seawater/freshwater intrusion at different times, which can be read in terms of the contrast between two opposing flows that compete to 'invade' the aquifer, and so is representative of the dynamics of the process.

The figures represent continuous alternation in time of the freshening and intrusion stages, and the respective reactions within the aquifer. Furthermore, representation of facies or sub-stages allows identification of the extent of the sector compromised by seawater intrusion in a salinized aquifer, which extends from the freshwater domains ($FW+f_4$) to the saltwater domains ($SW+ i_4$). The domain will be larger or smaller depending on how far along the process each phase is.

Table 3 shows the percentage of samples for each sub-stage in FwI and SwI for every sampling period. The three maps of Vinaroz Plain for the three sampling periods (Figures 7a, 7b and 7c) reveal that it is possible to identify variations in the position of the boundary between the intrusion and freshening fields, in time and space.

Table 3. Distribution of sub-stages (in %) in freshening and intrusion phases for each sample period.

	$FW+f_4$ (%)	f_3 (%)	f_2 (%)	f_1 (%)	i_1 (%)	i_2 (%)	i_3 (%)	$SW+i_4$ (%)	Total (%)	N
JULY 1990	29	5	5	5	5	10	19	24	100	21
NOVEMBER 1990	6	18	12	0	12	18	6	29	100	17
DECEMBER 1990	15	15	5	10	5	20	5	25	100	20
		freshening			intrusion					
		proximal ←		*distal*	*distal* →		*proximal*			

The varying positions of the sub-stages on the three dates examined are a sign of the dynamism of the process in Vinaroz Plain and it denotes what hydrochemical changes can be related to changes in the balance of the aquifer and the dynamics of the salinization from seawater intrusion. The aquifer goes through different stages in the space of a few months, as the maps from July and November 1990 show. The heatmaps show a fairly advanced freshening process in July 1990, a rather early freshening action in November 1990 (after a dry summer in which the salinization had advanced considerably), and an example of moderate rinsing in December 1992. It does not appear that the I-R/I^{i+} relationship has an important influence on the development of the freshening phases with respect to the intrusion phases. Judging from the heat-maps, both phases can reach full development.

Some areas of the aquifer stay virtually unchanged over time and, in this way, one can identify the main areas of recharge and the zones affected by salinization. On the Vinaroz Plain, the main recharge areas are located: in the N of the plain – from the Sierra del Montsià; in the W, from the northern part of the La Cenia-Tortosa Plain; and in the SW from the Sierra de Irta foothills. Meanwhile, seawater intrusion is identified along the coastal fringe. The salinized areas along the coast are near the two major towns of Vinaroz and Benicarló. These two restricted areas, where salinization is virtually constant through time, have been represented as corresponding to lateral saltwater intrusion; although the salinization could also be the result of 'upconing'.

One aspect that clearly stands out on the maps is the curvature of the boundary, which reflects the competition between the freshwater recharge and the intruding seawater. It defines the main recharge areas and the areas most salinized due to seawater intrusion.

In July, the boundary lies quite close to the coast and sub-stage FW+f_4 (associated with the most proximal facies) occupied a large proportion of the coastal plain. This suggests that, at this moment, recharge was important, the dominant freshening sub-stages was FW+f_4 (29%), against 5% for sub-stages f_3, f_2 and f_1. The curvature of the boundary indicates recharge zones that follow the watercourses of the river La Cenia to the north, and of the river Seco to the south. The aquifer is being recharged to a significant degree: the aquifer is in an advanced phase of freshening, which is rinsing the aquifer after a salinization. The most saline areas are restricted to the coastal fringe and are characterized by sub-stages i_3 and SW+i_4 (43%), which highlights that there was a significant development of this stage over preceding months. These proximal facies dominate over sub-stages i_2 and i_1 (15%), which represent the distal facies or the initial stages of intrusion (Table 3 and Figure 7a).

In contrast, in November 1990, the boundary is much further inland and salinization has reached quite a distance from the coast. The most salinized zones of the coast broadly coincide with the ones recognized in July of the same year; similarly with the areas of recharge. In the freshening phase, the proximal facies (f_3 and f_2, 30%) dominate. These proximal facies characterize quite an advanced phase of freshening, following a period of

salinization that was probably well developed. The intrusion extends from the coast inland, with similar percentages of the distal intrusion facies, i_2 and i_1, (30%) and the proximal ones (i_3 and SW+i_4; 35%) (see Table 3 and Figure 7b).

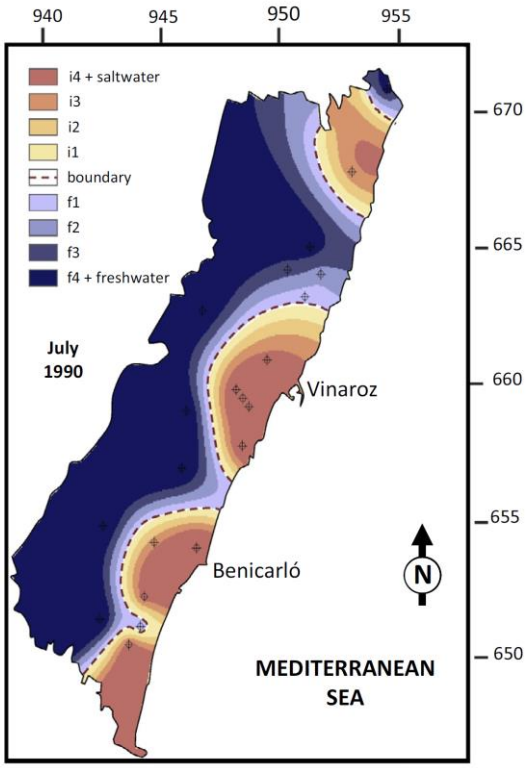

Figure 7a. Distribution of facies representing substages in the aquifer in July 1990.

The map corresponding to December 1992 (Figure 7c) reveals that the aquifer is again in a recharge phase that is slightly more advanced than the one recognised in November 1990, but less developed than in July 1990. It is characterized by a freshening phase that extends to areas quite close to the coast, and which is characterized by the sub-stages of proximal facies FW+f_4 and f_3 (30%). This contrasts with the 15% of the distal facies corresponding to sub-stages f_2 and f_1 (Table 3).

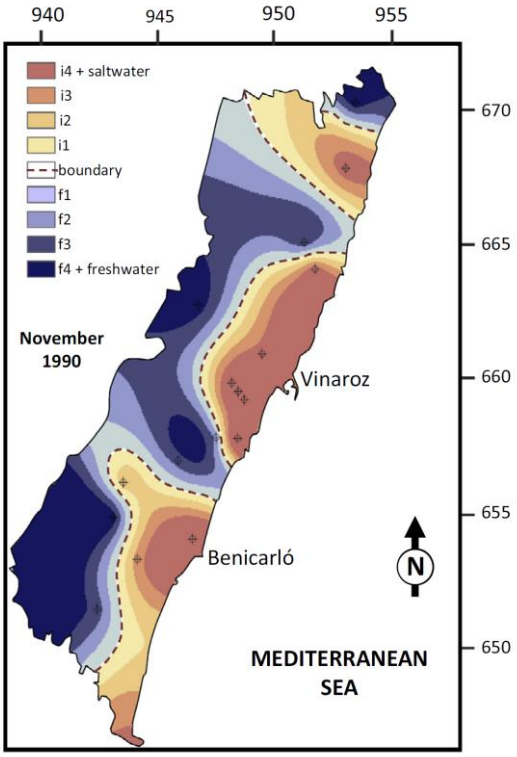

Figure 7b. Distribution of facies representing substages in the aquifer in November 1990.

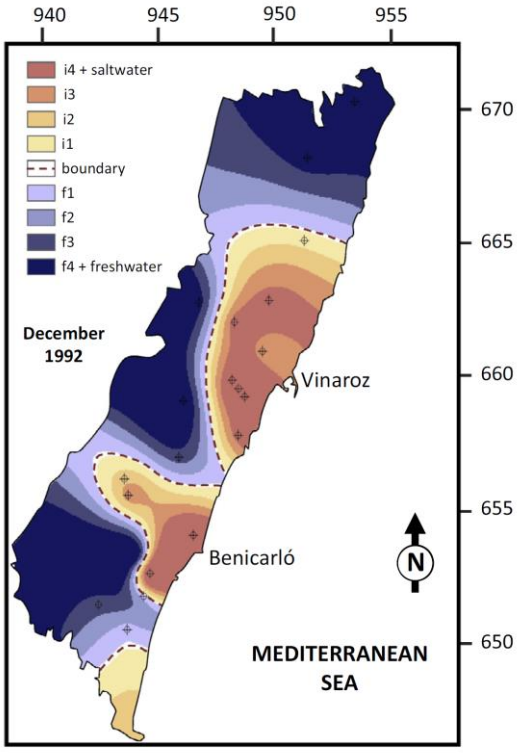

Figure 7c. Distribution of facies representing substages in the aquifer in December 1990.

The intrusion phase is confined to the coastal zone and is represented by 30% proximal intrusion facies (sub-stages SW+i_4 and i_3), and 25% distal facies (sub-stages i_2 and i_1). The main recharge areas are recognised by the freshening facies that are most proximal. In contrast to the earlier cases, the recharge that the aquifer normally receives (associated with the course of the river La Cenia), is not recognized at this moment. The absence of this freshwater flow allows salinization to extend NW from Vinaroz quite a long way from the coast.

The differences in hydraulic gradient commented earlier (shallower in the north and steeper in the south) could explain the differences in the development of the succession of facies between the northern and southern parts of the Plain. The maximum development of the sub-stages in the three figures (measured by the width of the area represented) seems to be in the north, in the vicinity of the river La Cenia; whilst in the south, particularly S of the town of Benicarló (coinciding with the steepest hydraulic gradient identified by the traces of the isopieze lines; Figure 1), the development of the sub-stages is more limited. The lower hydraulic gradient in the north, especially around the river La Cenia, could be facilitating the development of the ion exchange reactions, permitting the different sub-stages to be recognised. This can be attributed to the fact that these conditions facilitate the flow of groundwater, both fresh and salt-water. In other words, these conditions favour changes in the chemical composition of the water and the corresponding exchange reactions. In contrast, the higher hydraulic gradient values in the southern part will translate into the opposite conditions to the previous case, impeding groundwater flow and therefore ion exchange.

7. CONCLUSIONS

The study shows that hydrochemical variations can be read in terms of the pattern of seawater intrusion. The analysis of seawater-freshwater mixing and ion exchange reactions using the HFE-Diagram, and the quantification of results using the representation of their

spatial variation in GIS-maps, provides a useful tool to identify variations in the state of the aquifer in relation to seawater intrusion.

The application of the methodology in the pilot area of the Vinaroz Plain enables the main areas of recharge can be recognized, as well as the location of the more persistent salinized sectors, and the sectors where temporal variations are more evident. The method shows itself to be an easy and helpful tool, which provides quick and reliable information about the state and evolution of seawater intrusion in a coastal alluvial aquifer.

The satisfactory results suggest that the method could be applied to other aquifers and that it can be considered a useful tool for improving management of water resources in coastal areas, using only major ion chemistry.

Acknowledgements

The author thanks the review and constructive comments provided by an anonymous reviewer which helped to improve the quality of this manuscript; their help is gratefully acknowledged

For representing HFE-Diagram, Excel Macro software is available free by downloading directly from http://hidrologia.usal.es/HFE-D.htm or http://www.igme.es/HFE-D/HFE-D.htm (see Giménez-Forcada, E. Sánchez San Román, F.J. (2014). An Excel Macro to plot the HFE-Diagram to identify seawater intrusion phases. *Groundwater* 2014. DOI: 10.1111/gwat.12280).

REFERENCES

APHA - AWWA - WPCF, 1989. Standard Methods for the Examination of Water and Wastewater. 17th Edition. American Public Health Association, Washington DC.

Appelo, C.A.J., Postma, D., 2005 Geochemistry, Groundwater, and Pollution. A.A. Balkema, Rotterdam.

Appelo, C.A.J., Willemsen, A., 1987. Geochemical calculations and observations on salt water intrusions, I. Journal of Hydrology 94, 313-330.

Appelo, C.A.J., Willemsen, A., Beekman, H.E. Griffioen, J., 1990. Geochemical calculations and observations on salt water intrusions, II. Journal of Hydrology 120, 225-250.

Bear, A. H., 1999. Conceptual and Mathematical Modeling, Chapter 5. In: J. Bear et al., eds. Seawater Intrusion in Coastal Aquifers, 73-125. Kluwer Academic Publishers, The Netherlands.

Beekman, H.E., 1991. Ion chromatography of fresh- and seawater intrusion. Multicomponent dispersive and diffusive transport in groundwater. H.E. Beekman, Leiderdorp. The Netherlands.

Boluda, N., 1994. Estudio hidrogeoquímico de la intrusión marina. Simulación experimental y desarrollo de un modelo teórico. Ph.D. Department of Chemical Engineering. University of Alicante, Spain.

Boluda-Botella, N., Gomis-Yagües, V., Ruiz-Beviá, F., 2008. Influence of transport parameters and chemical properties of the sediment in experiments to measure reactive transport in seawater intrusion. Journal of Hydrology 357, 29– 41.

De Montety, V., Radakovitch, O., Vallet-Coulomb, C., Blavoux, B., Hermitte, D., Valles, V., 2008. Origin of groundwater salinity and hydrogeochemical processes in a confined coastal aquifer. Case of the Rhône delta, Southern France. Applied Geochemistry 23, 2337–2349.

Drever, J.I. 1988. The geochemistry of natural waters. Ed.: Prentice Hall.

Englewood Cliffs (U.S.A.)Fidelibus, M.D., Giménez, E., Morell, I., Tulipano, L., 1993. Salinization processes in the Castellon Plain aquifer (Spain). In: Custodio, E., Galofré, A. (Eds.), Study and Modelling of

Saltwater Intrusion into Aquifers. Centro Internacional de Métodos Numéricos en Ingeniería, Barcelona, pp. 267–283.

Giménez, E., Morell, I., 1988. La intrusión marina en los acuíferos costeros de la provincia de Castellón. In: Tecnología de la intrusión marina, TIAC´88, III, 99-109.

Giménez, E., 2003. Análisis de facies hidroquímica en el acuífero de la Plana de Vinaroz-Peñíscola, provincia de Castellón. Ábula 4, 19-28.

Giménez, E., Fidelibus, M.D., Morell, I., 1995. Metodología de Análisis de facies Hidroquímica aplicada al estudio de la intrusión marina en acuíferos detríticos costeros: Aplicación a la Plana de Oropesa, Castellón. Hidrogeología 11, 55-72.

Giménez-Forcada, E. , 2008. Caracterización hidrogeoquímica de los procesos de salinización en el acuífero detrítico costero de la Plana de Castellón, España. Agua Cultura y Medio Ambiente. Castellón, Spain.

Giménez-Forcada, E., 2010. Dynamic of seawater interface using hydrochemical facies evolution diagram. Ground Water 48 (2), 212–216.

Gomis, V., Boluda N., Ruiz, F., 1996.) Application of a model for simulating transport of reactive multispecies components to the study of the hydrogeochemistry of salt water intrusions. Journal of Contaminant Hydrology 22, 67-81.

Gomis-Yagües, V., Boluda-Botella, N., Ruiz-Beviá, F., 1997. Column displacement experiment to validate hydrogeochemical models of seawater intrusions. Journal of Contaminant Hydrology 29, 81-91.

Gomis-Yagües, V., Boluda-Botella, N., Ruiz-Beviá, F., 2000. Gypsum precipitation as an explanation of the decrease of sulphate concentration during seawater intrusion. Journal of Hydrology 228, 48–55.

Hoffmann G., Jouzel, J., Masson, V., 2000. Stable water isotopes in atmospheric general circulation models. Hydrological Processes, 14 (8), 1385–1406.

IGME, 1983. Mapa hidrogeológico de España. Hoja 48. Vinaroz. Escala 1:200.000. Serv. Publ. Mº Industria y Energía.

IGME, 1988. Atlas hidrogeológico de la provincia de Castellón. Diputación Provincial de Castellón, Servicio de Publicaciones. Castellón.

Kafri, U., Arad, A., 1979. Current subsurface intrusion of Mediterranean seawater. A possible source of groundwater salinity in the Rift Valley System, Israel. Journal of Hydrology 44, 267-287.

Lambrakis, N., Kallergis, G., 2001. Reaction of subsurface coastal aquifers to climate and land use changes in Greece: modelling of groundwater refreshening patterns under natural recharge conditions. Journal of Hydrology 245, 19-31.

Lambrakis, N., 2006. Multicomponent heterovalent chromatography in aquifers. Modelling salinization and freshening phenomena in field conditions Original Research Article. Journal of Hydrology 323 (1–4), 230-2436.

Manzano, M.S. 1993. Génesis del agua intersticial del acuitardo del Delta del Llobregat: origen de los solutos y transporte interactivo con el medio sólido. Ph.D. Technical University of Catalunya, Spain.

Martínez, D.E. Bocanegra, E.M., 2002. Hydrogeochemistry and cation-exchange processes in the coastal aquifer of Mar Del Plata, Argentina. Hydrogeology Journal 10, 393–408.

Masterson, J.P., Garabedian, S.P., 2007. Effects of sea-level rise on ground-water flow in a coastal aquifer system. Ground Water 45 (2), 209-217.

Melloul, A., Collin, M., 2006. Hydrogeological changes in coastal aquifers due to sea level rise. Ocean & Coastal Management 49 (5-6), 281-297.

Navarrete, P., Fabregat, V., Lopez-Geta, J.A., 1988. Evolución y estado actual de la intrusión marina en el litoral de la provincia de Castellón. Tecnología de la intrusión marina, TIAC´88, II, 111-128.

Pulido-Lebeuf, P., 2004. Seawater intrusion and associated processes in a small coastal complex aquifer (Castell de Ferro, Spain). Applied Geochemistry 19, 1517-1527.

Rutulis M, 1989. Groundwater drought sensitivity of southern Manitoba. Canadian Water Resources Journal 14, 18-33.

Xu, T., Samper, J., Ayora, C., Manzano, M. Custodio, E., 1999. Modeling of non-isothermal multi-component reactive transport in field scale porous media flow systems. Journal of Hydrology 214, 144–164.